# Facile Synthesis of Optically Functional, Highly Organized Nanostructures: Dye – Surfactant Complexes

**Charl F. J. Faul* and Markus Antonietti[a]**

**Abstract:** Multiply charged dye molecules can be precipitated from water by complexation with oppositely charged surfactants. It is shown that this complex formation occurs with 1:1 stoichiometry in a highly cooperative fashion. The resulting solids show either a gel-like or a supramolecular fibrillar morphology with a very high degree of order on the nanoscale, as evidenced by small-angle X-ray scattering and pleochroic behavior under plane-polarized light.

**Keywords:** cooperative phenomena · dyes/pigments · nanostructures · self-assembly · surfactants

## Introduction

Dye molecules are almost the ideal building blocks for supramolecular chemistry: they are easily available, have a number of functional groups, possess (because of their extended π system) a defined and regular shape and mutual interactions, and they have optical and electronic functions. This is reflected in a number of recent publications on the supramolecular organization of dyes with special substitution patterns and finding a very high degree of hierarchical complexity.[1–8]

The approach of the present publication is somewhat complementary: here we want to employ multicharged, water-soluble standard dye molecules and make them self-organizing by complexation with appropriate organic counterions, namely oppositely charged surfactants.

A similar mode of order formation is well known from polyelectrolyte – surfactant[9–11] and polyelectrolyte – lipid complexes[12] or from the H-bridge mediated supramolecular complexes between polar polymers and alkylphenols.[13, 14] It is well known from the literature (from the determination of binding isotherms)[15, 16] that the complexes are formed in a highly cooperative way.

Contrary to the more simple polymer – surfactant complexes, dye – surfactant complexes are expected to behave in a more complex manner due to the shaped nature of the oligoelectrolytic species, in contrast to the ill-defined molecular architecture of flexible polymer chains. It is therefore also expected to find mesoscopic order of an even higher degree than found for polyelectrolyte – surfactant complexes, because of this third competing energy contribution, the stacking of the π systems due to shape rigidity and electronic interactions. The complexation reaction, however, is expected to be rather simple since it is known that this counterion binding occurs in a strict 1:1 fashion,[17] and that the resulting product usually precipitates from water and can be isolated. Due to the amphiphilicity contributed by the surfactant, the π systems, ionic sites, and hydrophobic tails are expected to form or demix into three different subphases. The minimization of the packing and interface energy should therefore result in structural complexity with a high degree of supramolecular order even for standard dyes and surfactants.

In this investigation of a series of multiply charged azosulfonium dyes (see Scheme 1) with different standard cationic surfactants of varying length and tail number, we analyzed exemplarily the binding process of two dyes with dodecyltrimethylammonium chloride using a surfactant-selective electrode. This was used to characterize the spontaneous, cooperative formation of the complexes as well as their stoichiometry. Isolated solid complexes were then examined

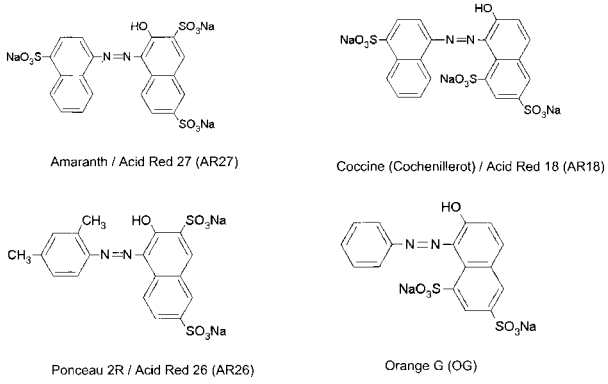


Scheme 1. Structures of the dyes used.

[a] Dr. C. F. J. Faul, Prof. Dr. M. Antonietti
Max Planck Institute of Colloids and Interfaces
Research Campus Golm, 14424 Potsdam-Golm (Germany)
Fax: (+49) 331-567-9502
E-mail: charl.faul@mpikg-golm.mpg.de

  0947-6539/02/0812-2764 $ 20.00+.50/0 

by small-angle X-ray scattering, electron microscopy, and differential scanning calorimetry to characterize the resulting supramolecular structure.

Finally, light microscopy revealed an exciting coupling between optical and structural properties, namely a very strong and close-to-perfect pleochroism of the fiber-like aggregates.

## Results and Discussion

In order to obtain more information on the binding process between the charged dyes and oppositely charged surfactants, binding isotherms were calculated and plotted as the degree of binding, $\beta$, versus the free-surfactant concentration. This was determined by potentiometric titration (by using a surfactant-selective electrode to determine free-surfactant concentrations) according to the standard methods for the determination of binding isotherms for polyelectrolyte and surfactant interactions, as detailed in references [15] and [16]. $\beta$ is defined, here in the case of oligoelectrolytic dye molecules, as the fraction of the total charged sites (from the dye) occupied by bound surfactants.

$$\beta = (C_{s,T} - C_{s,F})/C_{OE} = C_{s,B}/C_{OE} \quad (1)$$

with $C_{s,T}$ defined as the total surfactant concentration, $C_{s,F}$ as the free surfactant concentration, $C_{OE}$ as the concentration of charges on the oligoelectrolytic dye, and $C_{s,B}$ as the concentration of bound surfactant.

Figure 1 shows typical binding isotherms of the dyes Acid Red 27 (AR27, as an example of a triply charged species) and Orange G (OG, as an example of a doubly charged species) with dodecyltrimethylammonium chloride (DTAC). As can be seen from the figure, the binding of the surfactant to the dye takes place well below the critical micelle concentration (CMC) of the surfactant (20 mM in the case of DTAC). On the other hand, the interaction does not start at the same low free surfactant concentration as found in polyion–surfactant interactions, in which the point of interaction (the CAC, or critical aggregation concentration) is usually two to three orders of magnitude lower than the CMC.[18] This indicates that the free enthalpy of binding is lower for the dye–surfactant complexes.

The binding process is clearly cooperative, as can be seen from the steep initial curve of the isotherm. In the present case, the $\pi-\pi$ stacking interactions of the oligoelectrolytic azo-dye systems obviously replace the polymeric character (as found in the polyelectrolyte–surfactant systems) to generate the observed cooperative binding behavior. Therefore, binding involves more than one dye molecule; this already hints at the instantaneous formation of larger, common supramolecular aggregates. Binding also only takes place to an initial value of $\beta = 0.88$ in the case of AR27 and $\beta = 0.76$ in the case of OG. The calculation of $\beta$ assumes the presence of a pure dye with three charges (or two in the case of OG). $\beta$-Values lower than 1 may therefore be due to impurities in the used crude dye-stuff.

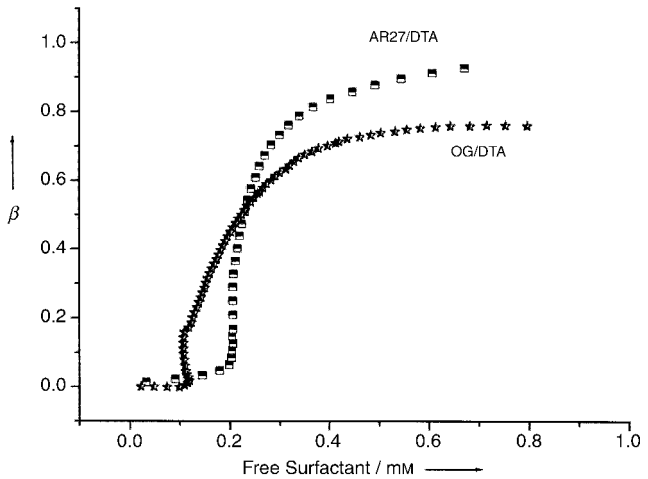


Figure 1. Binding isotherms of AR27 and OG with DTAC, ▪: AR27/DTA; stars: OG/DTA.

In order to evaluate the degree of cooperativity, the values of the binding constant, $K_u$, and the cooperativity parameter, $u$, are evaluated. From the Zimm–Bragg theory for helix–coil transitions,[19] and further modifications by Schwarz,[20] and Satake and Yang[21] to describe the cooperative binding of small ions to polyions, it is possible to calculate these values from the following equations:

$$(C_{s,F})_{0.5} = (K_u)^{-1} \quad (2)$$

$$(d\beta/d\ln C_{s,F})_{0.5} = u^{1/2}/4 \quad (3)$$

here $(C_{s,F})_{0.5}$ is defined as the free-surfactant concentration at $\beta = 0.5$, and $(d\beta/d\ln C_{s,F})_{0.5}$ as the slope of the binding isotherm at $\beta = 0.5$.

The values obtained from the titration of the dyes with DTAC, together with physical properties of the complexes formed are listed in Table 1. It is very interesting to note that, in the first part of the binding process, the isotherm curve has a negative slope. This indicates that as the cooperative process of binding is started, free surfactant from the solution is incorporated into the complexes, causing a slight decrease of this species. This is typical for nucleation processes, and

Table 1. Material properties and values of $K_u$ and $u$ as obtained from the bindings isotherms.

| Surfactant | Sample | Appearance | $K_u$ | $u$ |
|---|---|---|---|---|
| DTAC | AR27 | needle-like precipitate strongly pleochroic | 5.56 | 600 |
| | OG | needle-like precipitate, pleochroic | 4.58 | 65 |
| | AR18 | gel—birefringent with shear | | |
| | AR26 | needle-like material, pleochroic | | |
| CTAB | AR27 | birefringent Gel | | |
| | OG | gel-like material containing needle-like structures, needles pleochroic | | |
| | AR18 | Gel-like, containing solid birefringent material | | |
| | AR26 | Needle-like material (shape not well defined), pleochroic | | |
| DiDAB | AR27 | Gel-like material separating from solution | | |
| | OG | Gel-like material separating from solution | | |

  0947-6539/02/0812-2765 $ 20.00+.50/0 

indicates that the described complexes are on the borderline between molecular supramolecular assemblies and nanostructured solid-state materials. Due to this, the $u$ values and the binding isotherms are also afflicted with a minor systematic uncertainty, since nucleation can depend on external parameters.

The isolated precipitate from two points on the titration curve (1:3 surfactant to charge ratio complex and a 1:1 charge ratio) for the AR27–DTA complex was investigated by means of elemental analysis. The results showed that there was no difference in the elemental ratios, thus binding is indeed given by charge stoichiometry, and no significant physical adsorption of surfactant onto the precipitate takes place. In Na and Cl determinations, 0.042 wt% $Na^+$ and 0.090 wt% $Cl^-$ was found. This corresponds theoretically to one Na ion every 46 repeat units (e.g. one uncomplexed charge site per 46 dye molecules), and one adsorbed $Cl^-$, for example through an extra adsorbed surfactant molecule, bound per every 31 repeat units. This means that the as-precipitated complex is essentially a rather pure 1:1 species.

It must be noted that the precipitated material, as all Coulomb complexes, can—after isolation—be redissolved in water by addition of high amounts of salts or polyelectrolytes of similar charge as the dye (note that the binding to the polyelectrolyte is stronger, so that competitive binding liberates the dye from the complex). This could therefore be used for the convenient purification of water-soluble dyes by cyclic complexation with surfactant molecules.

In order to investigate the thermal behavior of the complexes, thermal analyses (thermogravimetric analysis: TGA and differential scanning calorimetry: DSC) were performed on purified dried precipitates. TGA indicated that the complexes started to degrade at temperatures below 300 °C. DSC analyses were then performed to ascertain whether any phase transitions could be detected below the determined degradation temperatures.

The DSC trace of the AR27/DTA complex is shown in Figure 2a. From the DSC trace it can be seen that the precipitated complex material is crystalline/liquid crystalline in nature. In the first heating curve, two transitions at 9.4 and 13 °C can be observed, which can be attributed to melting of the partially crystalline side chains of the surfactant subphase of the complex. A broad transition at approximately 80 °C was also observed, which we identify as a liquid crystalline phase transition, since birefringence is preserved above this temperature. A further sharp endothermic transition is observed at 250 °C, which is attributed to the clearing point or the transition to the isotropic liquid state.

Similar behavior is found for all the complexes, and, depending on dye and surfactant, can become highly complex. Figure 2b shows the DSC trace from the OG/DiDA complex, which exhibits no less than seven endothermic transitions below 200 °C in the first heating curve. The second heating curve, however, shows just two reversible transitions at 149.5 and 172 °C, respectively.

Temperature-dependent X-ray measurements of this compound are shown in Figure 3a. Evidently, the two low-temperature phases are highly ordered and show a large number of overlapping or related peaks, whereas the high-

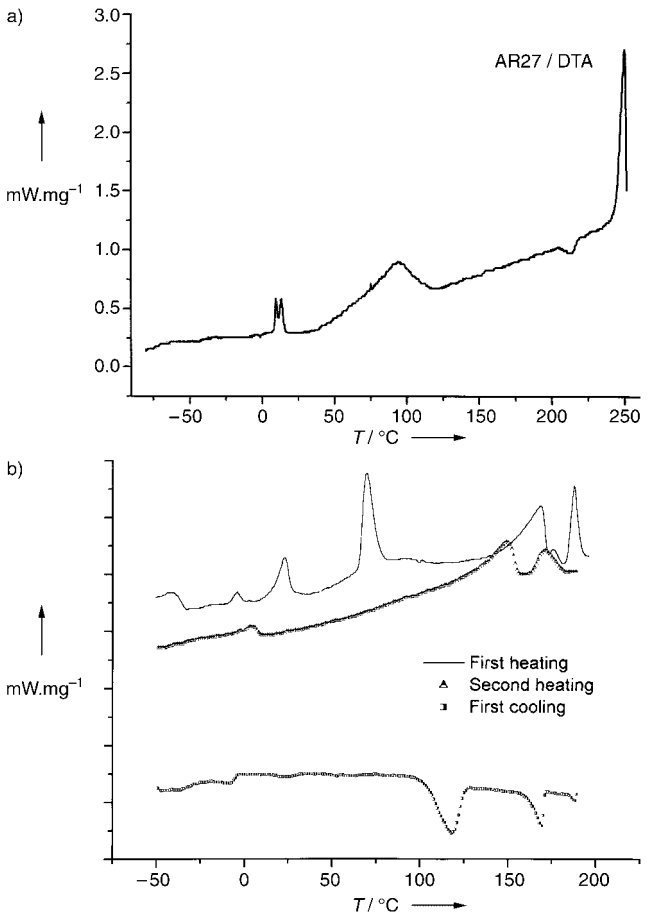


Figure 2. DSC traces from the complexes a) AR27/DTA and b) OG/DiDA.

temperature phase is clearly weakly ordered liquid crystalline. Additional polarized-light microscopy shows that the phases observed at 130 °C and 50 °C have very similar, fan-like textures, that is, they belong to the same family of highly ordered structures, presumably a smectic or two-dimensional crystalline order. The presence of the additional peaks at smaller scattering vectors in the low-temperature phase ($s = 0.227\ nm^{-1}$), probably originates from higher dimensional order (ABAB stacking). As a result of the observed complexity, full elucidation of the structure model falls outside the scope of this investigation and is the subject of ongoing work.[22]

The powder small-angle X-ray (SAXS) diffractogram of the AR27/DTA complex is shown in Figure 3b. The formed complexes obviously exhibit very high mesomorphic order on the Ångström and nanometer scale, as can be seen from the high number of narrow peaks in the SAXS diffractogram. It is known from the mesomorphic states of dyes that they form, for example, hexagonally packed columnar aggregates or rigid multilayer structures (see ref. [8]). From the SAXS diffractogram in Figure 3b, for example, it is clear that the diffraction patterns are not consistent with any known basic phase patterns. The elucidation of the exact phase structure relies on the presence of a single crystal or monodomain, and is currently under investigation.

  0947-6539/02/0812-2766 $ 20.00+.50/0 *Chem. Eur. J.* **2002**, *8*, No. 12

The macroscopic appearance of the as-precipitated complexes is best characterized by light microscopy. It can be seen that the high order observed in the SAXS diffractogram is also reflected in the macroscopic optical properties. Figure 4 shows the same set of fiber-like aggregates illuminated with plane polarized light, tilted by an angle of 90° between the pictures. Almost perfect pleochroism is obtained, that is, the crystals are transparent in one orientation whereas they are colored in the one perpendicular. This means that the transition moment of all dye molecules is oriented in the same direction (perpendicular to the fibers), and that orientation of the macroscopic fiber also leads to perfect control of the orientation of the molecular dye unit.

## Conclusion

In summary, the synthesis of a functional, supramolecular organic composite material by simple precipitation of charged dyes with oppositely charged surfactants has been described. Binding occurs at least very close to a 1:1 stoichiometry with respect to the number of charges and well below the CMC of the surfactant. The resulting structures are highly organized crystals or thermotropic liquid crystals (depending on the system and temperature), as revealed by X-ray scattering and calorimetry. The simplicity of the synthesis, as well as their optical and dielectric properties, makes these complexes promising for a number of scientific investigations and possible applications.

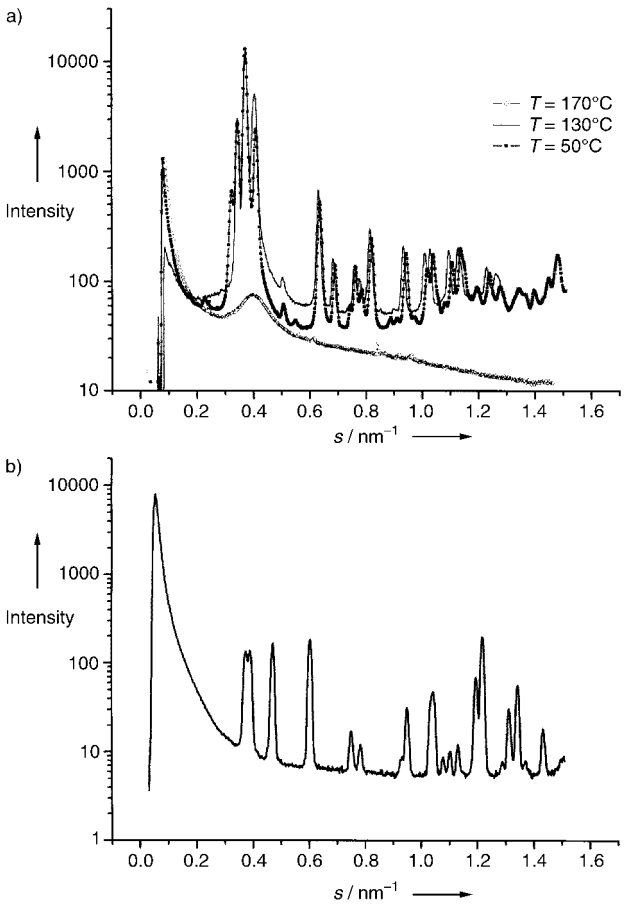


Figure 3. Temperature-dependent small-angle X-ray diffractograms of a) OG/DiDA, b) AR27/DTA. ——□——: $T = 170\,^{\circ}C$, ——: $T = 130\,^{\circ}C$, ——■——: $T = 50\,^{\circ}C$.

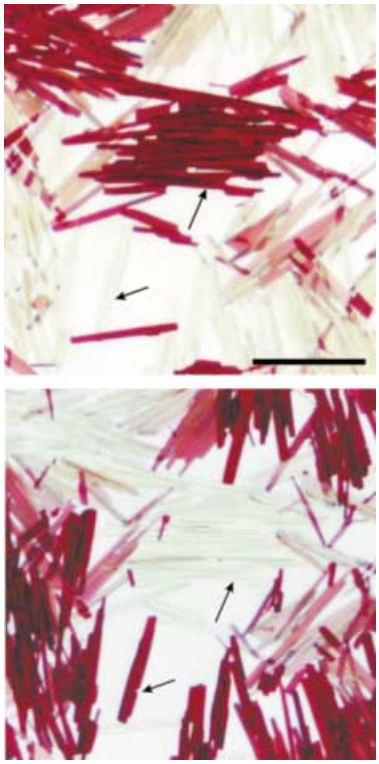

Figure 4. Fiber-like aggregates from the complex AR27/DTA as illuminated with plane-polarized light. The figures are tilted by an angle of 90° with respect to each other; this shows the almost perfect pleochroism over the full length of the aggregates. The arrows point to the same fiber or groups of fibers. Scale bar = 50 μm.

## Experimental Section

**Materials**: Amaranth/Acid Red 27 (AR27), Orange G (OG), and dodecylammonium chloride (DTAC) from Fluka;, New Coccine/Acid Red 18 (AR18, dye content ≈75%), hexadecyltrimethylammonium bromide (CTAB), and didodecyldimethylammonium bromide (DiDAB) from Aldrich; and Ponceau 2R/Acid Red 26 (AR26, dye content ≈80%) from Sigma were used as received. The structures of the dyes are shown in Scheme 1. Deionized water (resistance > 18 MΩ) was used to prepare all solutions.

**Example synthesis of a dye – surfactant complex**: For production of a 1:1 charge ratio complex, the dye AR27 (0.5 g, 0.827 mmol) was dissolved in deionized water to yield a 2% solution. A 2% surfactant solution was prepared by dissolving DTAC (0.654 g, 2.48 mmol) in deionized water to yield a 2% solution. The surfactant was added in 0.5 mL aliquots at 3 minute intervals with stirring. The precipitated complex was centrifuged and washed with deionized water (3 × 30 mL) to remove the unbound counter ions. The resulting cleaned complex was dried under vacuum at room temperature.

**Analysis**: In order to determine binding isotherms, potentiometric titrations were performed with either a 702 SM Titrino or 716 DMS Titrino potentiometer in conjunction with a 765 Dosimat (all from Metrohm). The dosing of surfactant and dye solutions was controlled by Tinet Version 2.4 Titration Software (Metrohm). Dye was added after each addition of surfactant to keep the concentration of dye constant in the measured solution. An "Ionic Surfactant Electrode" (Metrohm) was used as a surfactant-selective electrode, in conjunction with a Ag/AgCl reference electrode (Metrohm). All titrations were performed in a thermostated cell

(25.0 °C ±0.1 °C) with stirring. The waiting period after addition of solutions was set to be 180 s in order to allow equilibration of the solution temperature and the electrode after each addition.

*In a typical titration*, a dye solution of AR27 (1.5 mM, 4.5 mM with respect to charges present) was prepared in the titration cell by addition of a concentrated dye solution and subsequent dilution with water. All additions were performed using the 765 Dosimat to ensure high precision and repeatability in the preparation of the solutions.

*Small-angle X-ray (SAXS)* curves were recorded by means of a Kratky camera and a rotating anode instrument with pinhole collimation. A Nonius rotating anode ($P = 4$ kW, $Cu_{K\alpha}$) and an image plate detector system were used with the pinhole system. With the image plates placed at a distance of 40 cm from the sample, a scattering vector range from $s = 0.05$ – 1.6 $nm^{-1}$ was available ($s = 2\sin\theta/\lambda$, $2\theta$ scattering angle, $\lambda = 0.15418$ nm). The samples were irradiated for 18 h in order to reduce the noise level and to obtain a sufficiently high scattering intensity. 2D diffraction patterns were transformed into a 1D radial average of the scattering intensity.

*Wide-angle X-ray scattering (WAXS)* measurements were performed on a Nonius PDS 120 powder diffractometer in transmission geometry. A FR 590 generator was used as the source of $Cu_{K\alpha}$ radiation. Monochromatization of the primary beam was achieved by means of a curved Ge crystal. Scattered radiation was measured by using a Nonius CPS 120 position-sensitive detector. The resolution of this detector in $2\theta$ is 0.018°.

*Differential scanning calorimetry (DSC)* was performed on a Netzsch DSC 200 calorimeter. The samples were examined at a scanning rate of 10 K $min^{-1}$ by applying two heating and one cooling cycle.

*Na analyses* were performed by inductively coupled plasma optical atomic emission spectrometry by using an Optima 3000 ICP-OES (Perkin Elmer). The amount of $Cl^-$ was determined according to Schöninger's method, followed by potentiometric titration with silver nitrate.

## Acknowledgement

We thank the Max Planck Society and the Fund of the German Chemical Industry for financial support. Help with the X-ray measurements by Bernd Smarsly and Ingrid Zenke, and technical help by Carmen Remde, Irina Shekova, and Rona Pitschke are gratefully acknowledged.

[1] F. Würthner, C. Thalacker, S. Diele, C. Tschierske, *Chem. Eur. J.* **2001**, *7*, 2245.
[2] K. Pieterse, P. A. van Hal, R. Kleppinger, J. A. J. M. Vekemans, R. A. Janssen, E. W. Meijer, *Chem. Mater.* **2001**, *13*, 2675.
[3] F. Würthner, C. Thalacker, A. Sautter, W. Schärtl, W. Ibach, O. Hollricher, *Chem. Eur. J.* **2000**, *6*, 3871.
[4] H. von Berlepsch, C. Böttcher, A. Ouart, C. Burger, S. Dähne, S. Kirstein, *J. Phys. Chem. B* **2000**, *104*, 5255.
[5] H. von Berlepsch, C. Böttcher, A. Ouart, M. Regenbrecht, S. Akari, U. Keiderling, H. Schnablegger, S. Dähne, S. Kirstein, *Langmuir* **2000**, *16*, 5908.
[6] T. Imae, L. Gagel, C. Tunich, G. Platz, T. Iwamoto, K. Funayama, *Langmuir* **1998**, *14*, 2197.
[7] Ch. Hahn, I. Spring, C. Thunig, G. Platz, A. Wokaun, *Langmuir* **1998**, *14*, 6871.
[8] G. J. T. Tiddy, D. L. Mateer, A. P. Ormerod, W. J. Harrison, D. J. Edwards, *Langmuir* **1995**, *11*, 390.
[9] M. Antonietti, J. Conrad, *Angew. Chem.* **1994**, *106*, 1927; *Angew. Chem. Int. Ed. Engl.* **1994**, *33*, 1869.
[10] M. Antonietti, J. Conrad, A. Thünemann, *Macromolecules* **1994**, *27*, 6007.
[11] M. Antonietti, C. Burger, J. Effing, *Adv. Mater.* **1995**, *7*, 751.
[12] M. Antonietti, A. Wenzel, A. Thünemann, *Langmuir* **1996**, *12*, 2111.
[13] J. Ruokolainen, M. Torkkeli, R. Serimaa, S. Vahvaselkä, M. Saariaho, G. ten Brinke, O. Ikkala, *Macromolecules* **1996**, *29*, 6621.
[14] J. Ruokolainen, G. ten Brinke, O. Ikkala, *Macromolecules* **1996**, *29*, 3409.
[15] K. Hayakawa, J. P. Santerre, J. T. C. Kwak, *Macromolecules* **1983**, *16*, 1642.
[16] K. Hayagawa, J. T. C. Kwak, *Phys. Chem.* **1983**, *87*, 506.
[17] P. Mukerjee, K. J. Mysels, *J. Am. Chem. Soc.* **1955**, *77*, 2937.
[18] E. D. Goddard, *Colloids Surf.* **1986**, *19*, 301.
[19] B. H. Zimm, J. K. Bragg, *J. Chem. Phys.* **1959**, *31*, 526.
[20] G. Schwarz, *Eur. J. Biochem.* **1970**, *12*, 442.
[21] I. Satake, J. T. Yang, *Biopolymers* **1976**, *15*, 2263.
[22] Y. Guan, M. Antonietti, C. F. J. Faul, *Langmuir*, in press.

Received: October 22, 2001 [F3627]

  0947-6539/02/0812-2768 $ 20.00+.50/0 